Synthesis, characterization and magnetism of monodispersed water soluble palladium nanoparticles†

Eugenio Coronado,*[a] Antonio Ribera,*[a] Javier García-Martínez,[b] Noemi Linares[b] and Luis M. Liz-Marzán[c]

Received 1st July 2008, Accepted 22nd September 2008
First published as an Advance Article on the web 24th October 2008
DOI: 10.1039/b811190a

Water soluble, monodispersed Pd nanoparticles with a narrow particle size distribution have been successfully synthesized by controlled reduction of $[PdCl_4]^{2-}$. The resulting aqueous colloids are stable over extended periods of time and can be prepared at high nanoparticle loading (20 g/L of Pd) with no agglomeration. The size of the nanoparticles can be reduced from the nanometer (*ca.* 3.5 nm) to the sub-nanometer size range (*ca.* 0.9 nm). Detailed magnetic characterization indicated that the larger, 3.5 nm nanoparticles show ferromagnetic properties at room temperature, while the sub-nanometric ones lose this magnetic behavior.

Introduction

Metal colloids have been known for a long time.[1] Current attention on nanotechnology has attracted renewed interest toward nanoparticles from both fundamental and practical points of view. Preparation, structural determination, study of the properties and exploration for diverse applications of nanosized materials are hot research topics. Fine metal nanoparticles have applications in areas such as catalysis, information storage, biological and chemical sensing, and opto-electronics due to their size-dependent optical, electrical and electronic properties.[2–8]

Most of these applications are strongly dependent on the size of the nanoparticle. Currently, one of the main objectives is to produce nanoparticles as monodispersed and small as possible.[9] Unfortunately, as the size of the nanoparticle gets smaller, the preparation becomes more challenging because of their tendency to aggregate and reduce surface tension. For this reason, many research groups have focused their efforts on the preparation of monodispersed nanosize materials by controlling both the nucleation and growth of the particles.

Since the pioneering article by Faraday on the preparation of colloidal gold,[1] a plethora of methods for the preparation of nanoparticles have been described including metal evaporation,[10,11] pyrolysis,[12–16] liquid–solid–solution (LSS),[17] vapour–liquid–solid (VLS) growth,[18–20] plasma-chemical reduction[21] and wet chemistry.[22] Considering the latter category, metal reduction in boiling sodium citrate aqueous solution is one of the most popular methods for preparing nanoparticle suspensions.[23–26] Another extensively used method is the so-called two-phase reduction method.[27,28] In this case the metal precursor is dissolved in water and transferred into the organic (toluene) phase by means of tetraoctylammonium bromide (TOAB). The metal is reduced by an aqueous solution of sodium borohydride, TOAB acting as the capping agent. Alternatively, thioalkanes and aminoalkanes can also be used as very efficient capping agents.[29–32] The third extensive group of wet chemistry methods comprises those in which the reduction of metal salts is performed by organic solvents, such as ethanol,[33,34] N,N-dimethylformamide,[35] or ethylene glycol and other polyols.[36–39]

Herein, we describe a simple method to prepare monodisperse nanoparticles in toluene, focusing in particular on those with sub-nanometer size. This involves a slight variation of the two-phase method, using TOAB as both phase transfer agent to transport the metal salt from the aqueous phase into toluene, and as capping agent. Additionally, we show that these Pd nanoparticles can be transferred from toluene to an aqueous solution using 4-dimethylaminopiridine (DMAP) as transfer agent,[28] without observing any increase in particle size. Finally, we present a detailed study of the magnetic properties of these nanoparticles.

Experimental

All chemicals used were of analytical grade. Sodium tetrachloropalladate was purchased from Pressure Chemical Co., sodium borohydride and 4-dimethylaminopyridine (DMAP) from Sigma-Aldrich and tetraoctylammonium bromide (TOAB) and toluene from Fluka. UV-Vis spectra were recorded with an Agilent 8453 UV-Vis spectrophotometer (0.1 nm resolution). The as synthesised samples were diluted (0.4 mL of fresh Pd nanoparticles in toluene were diluted up to 10 mL with toluene) in order to collect the UV-Vis spectra. TEM studies were carried out using a JEOL JEM-2010 instrument operating at an accelerating voltage of 200 kV. Several drops of the Pd suspensions were placed on the TEM lacey formvar/carbon grids and then air dried at room temperature for several hours. The digital analysis of the TEM micrographs and particle size determination was carried out using DigitalMicrograph™ 3.6.1. by Gatan. Thermogravimetric analyses were performed, over solid palladium

[a]*Instituto de Ciencia Molecular, Universidad de Valencia, Edificios Institutos de Paterna, Poligono La Coma s/n, E-46980 Paterna, Spain. E-mail: antonio.ribera@uv.es; Fax: (+34)963543273; Tel: (+34)963544419*
[b]*Departamento de Química Inorgánica, Universidad de Alicante, E-03690 Alicante, Spain*
[c]*Departamento de Química Física y Unidad Asociada CSIC, Universidade de Vigo, E-36310 Vigo, Spain*

† Electronic supplementary information (ESI) available: Magnetic hysteresis loops for Pd nanoparticles (sample A) at 2, 10, 100, 200 and 500 K. See DOI: 10.1039/b811190a

nanoparticle samples (obtained as described in the synthesis section), in air using a Mettler Toledo TGA/SDTA 851e. FT-IR spectra of solid palladium nanoparticles diluted in KBr were collected in a Nicolet 5700 FT-IR spectrometer from Thermo Electron Corporation. HRTEM measurements were carried out with a JEOL JEM-2010F instrument operating at an accelerating voltage of 200 kV. Fourier transformation was performed to obtain the reciprocal-space representation, which corresponds to the diffractogram of the corresponding image. The samples were prepared by dipping carbon coated copper grids in the palladium nanoparticles solution. X-Ray photoelectron spectra (XPS) were acquired with a VG-Microtech Mutilab 3000 spectrometer equipped with a hemispherical electron analyzer and a Mg Kα (h = 1253.65 eV; 1 eV = 1.6302×10^{-19} J), 300 W X-ray source. The solid palladium nanoparticle samples were pressed into a small Inox cylinder, mounted on a simple rod placed in a pre-treatment chamber and subsequently transferred to the analysis chamber. Before recording the spectra, the sample was maintained in the analysis chamber until a residual pressure of *ca.* 5×10^{-7} Nm^2 was reached. The spectra were collected at a pass energy of 50 eV. The intensities were estimated by calculating the integral of each peak, after subtracting the S-shaped background, and fitting the experimental curve to a combination of Lorentzian (30%) and Gaussian (70%) lines. All binding energies were referenced to the C 1s line at 284.6 eV, which provided binding energy (BE) values with an accuracy of $\pm$0.2 eV. X-Ray diffraction data were collected on a Seifert XRD 3003 TT (Bragg–Brentano geometry) powder diffractometer (Cu Kα radiation (λ = 1.54056 Å)). All the magnetic measurements were carried out powdered samples with a magnetometer (Quantum Design MPMS-XL-5) equipped with a SQUID sensor. Variable temperature susceptibility measurements were carried out on powdered samples in the 2–300 K temperature range at magnetic fields of 0.1 T. The diamagnetism from the holder was corrected by measuring the empty holder under the same conditions (magnetic field and temperature) used for the measurement of the Pd nanoparticles. Diamagnetism from the nanoparticles was also corrected taking into account the amount of capping agent and solvent surrounding the nanoparticles derived from thermal analysis. Isothermal magnetization measurements were collected in the H = 0–5 T field range at 2–300 K temperature range. The hysteresis studies were performed between 5 and -5 T, within the 2–300 K temperature range, cooling the samples at zero field.

Pd nanoparticles synthesis

The Pd nanoparticles were obtained by reduction of $[PdCl_4]^{2-}$ with $NaBH_4$, and subsequent stabilization with tetraoctylammonium bromide (TOAB ($N(C_8H_{17})_4Br$) used as a capping agent. The method is a variation of those proposed by the Brust and Caruso groups.[27,28] In a typical synthesis, 15 mL of a 30 mM aqueous solution of Na_2PdCl_4 was mixed with 40 mL of a 50 mM TOAB solution in toluene. Two hours later the transfer of the $[PdCl_4]^{2-}$ from the aqueous solution to the organic phase was completed as revealed by the red-brown color of the organic phase due to the $[PdCl_4]^{2-}$/TOAB complex. The colourless water phase was disposed and the toluene phase dried with Na_2SO_4. Then, 11.4 mL of a freshly prepared 0.1 M $NaBH_4$ aqueous solution was slowly added, keeping the mixture under vigorous stirring. The mixture was gently stirred overnight and, after removing the water phase, the organic phase was washed with 40 mL of a 0.1 M H_2SO_4 solution, 40 mL of a 0.1 M NaOH solution, and finally three times with 40 mL of dionized water. To remove the remaining water, the organosol was finally dried over anhydrous Na_2SO_4. Palladium nanoparticle samples were obtained by mixing 40 mL of the organosol with 1 L of ethanol and kept for 24 h at -18 °C. The fine black precipitate was collected by centrifugation at 12000 rpm and washed with ethanol.

With the aim of obtaining a homogeneous size distribution, especially with an average size in the nanometer range, the experimental conditions were systematically varied by altering some experimental parameters: i) capping agent concentration from 25 mM to 100 mM TOAB solution; ii) reducing agent concentration from 0.1 M to 1.2 M $NaBH_4$ solution; iii) water content in the $[PdCl_4]^{2-}$ toluene solution from 0 and 500 μL; iv) stirring rate from 400 to 1600 rpm.

Particle sizes in the range between 0.9 and 3.5 nm were obtained by systematically varying the above parameters.

Pd nanoparticle transfer from toluene to the water phase

This step was carried out following the procedure developed by Gittins and Caruso.[28] An aqueous 0.1 M DMAP solution was added to the as-prepared Pd nanoparticles in toluene, and the mixture was stirred for two hours. The conditions to perform the complete transfer of the Pd nanoparticles into the aqueous phase were studied. In a typical transfer reaction, 10 mL of the aqueous 0.1 M DMAP solution was mixed with 40 mL of the Pd nanoparticles colloid in toluene. To obtain a highly concentrated Pd hydrosol, the amount of DMAP solution was decreased to 2.5 mL.

Results and discussion

Controlling Pd nanoparticle size in toluene solution

Highly monodispersed Pd nanoparticles were prepared in toluene phase, on the basis of the methods previously developed by the Schiffrin[27] and Caruso[28] groups. This procedure ensures three important advantages: (i) Pd nanoparticles prepared in toluene instead of water show lower agglomeration, better particle size distribution, and smaller average size; (ii) tetraoctylammonium acts as both a phase transfer agent (quantitatively transferring tetrachloropalladate from water into toluene) and a capping agent (efficiently preventing nanoparticle growth and agglomeration); (iii) the non-covalent interaction between the Pd nanoparticles and tetraoctylammonium enables us to easily replace the capping agent.

A systematic study of the experimental parameters involved in the reduction of $[PdCl_4]^{2-}$ to Pd nanoparticles in toluene was carried out with the aim of both decreasing the nanoparticle size and narrowing down the particle size distribution. We studied the influence of the following parameters: i) capping agent concentration; ii) reducing agent concentration; iii) water content in the toluene solution; iv) stirring rate during the reduction. We found that the two key parameters to obtain small nanoparticles with a narrow particle size distribution are the concentration of the capping agent and the stirring rate used during the reduction of the Pd precursor in toluene. An optimal value for the capping

agent concentration around 50 mM was estimated. On the other hand, we observed that the higher the stirring rate, the smaller the particle size. This trend can be understood considering that the reduction from Pd(II) to Pd(0) in two-phase systems, like the one used herein, takes place at the phase boundary (organic to aqueous). Consequently, the stirring rate, which controls the size of the water droplets formed in the toluene/water mixture, has a dramatic effect on the size of the palladium nanoparticles.

By controlling these parameters we were able to obtain Pd nanoparticles with sizes between 0.9 nm and 3.5 nm. We focus in what follows on two representative samples: one, sample A, is formed by sub-nanometer particles with very small size and narrow particle size distribution, 0.9 ± 0.2 nm. This sample was obtained with the highest stirring rate of 1600 rpm and a capping agent concentration of 50 mM. A TEM micrograph of sample A is shown in Fig. 1. Both the small size and narrow size distribution of this sample are evident from this image. The other representative sample, sample B, comprises nanoparticles of larger sizes, 3.5 ± 0.5 nm and was obtained with lower stirring rate of 200 rpm and capping agent concentration of 25 mM. A TEM micrograph of sample B is also shown in Fig. 1 (bottom).

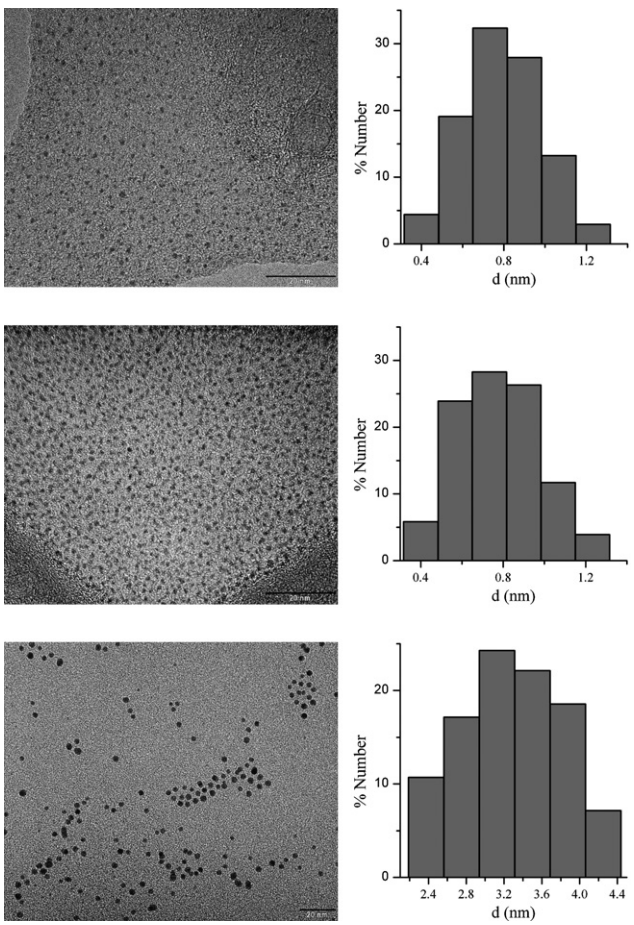

Fig. 1 Transmission electron micrograph of sub-nanometer (sample A) and 3.5 nanometer (sample B) palladium particles (top and bottom respectively) prepared by reduction of $[PdCl_4]^{2-}$ with $NaBH_4$ in toluene. (Middle) Sample A nanoparticles after transfer into the aqueous phase. The scale bar represents 20 nm.

Phase transfer of Pd nanoparticles from toluene into water

To transfer the Pd nanoparticles from toluene into the water phase we used an aqueous 0.1 M DMAP solution. As described elsewhere,[28] the neutral/zwitterion equilibrium of the DMAP molecule allows for a fast and efficient transfer of the metal nanoparticles (see Fig. 2) from toluene (neutral DMAP/Pd nanoparticle) into the water phase (zwitterion DMAP/Pd nanoparticle).

The nanoparticle transfer step can be used to either dilute or concentrate the Pd nanoparticles in the aqueous phase. Thus, when the volume of water is very small compared with that of toluene (1:16), monodispersed aqueous Pd nanoparticle suspensions with concentrations as high as 20 g of Pd/L can be reached. Thus, this procedure allows transfer of the Pd nanoparticles from toluene into the water phase, controlling the nanoparticle concentration during the phase transfer and without any change in the particle size, particle size distribution or stability, which is of great importance for further uses of these nanoparticles, like for example their incorporation into silica matrices.

Structural and spectroscopic characterization of palladium nanoparticles

Spectroscopic properties. The UV-Vis spectrum of $[PdCl_4]^{2-}$/TOAB in toluene shows a clear absorption band centred at 340 nm (Fig. 3) arising from a d–d transition. This band disappears when $[PdCl_4]^{2-}$ is reduced with $NaBH_4$ (Fig. 3) and the whole spectrum exhibits a broad, continuous absorption which can be matched to the spectrum of Pd nanoparticles reported in the literature.[40] Notice that, in contrast to what was found in colloidal dispersions of other noble metal nanoparticles, the UV-

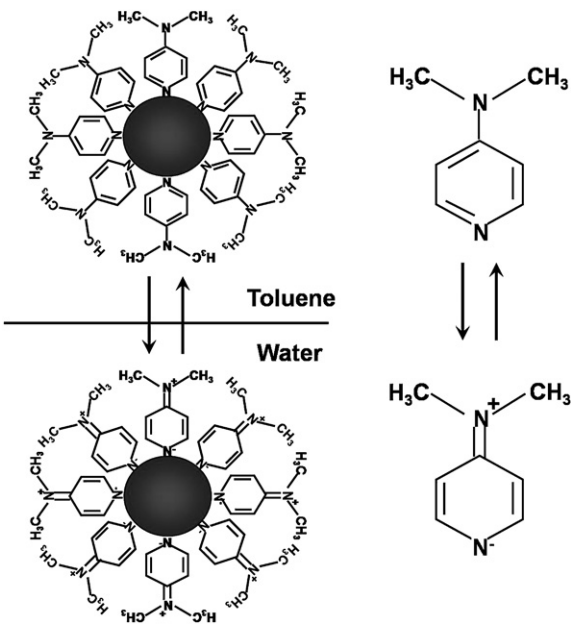

Fig. 2 Scheme of the experimental procedure used to transfer the Pd nanoparticles prepared in toluene into the aqueous phase. The phase transfer agent, dimethylaminopyridine (DMAP), neutral in the organic phase, is able to quantitatively extract the nanoparticles into the aqueous phase, where it is present as its zwitterion tautomeric form.

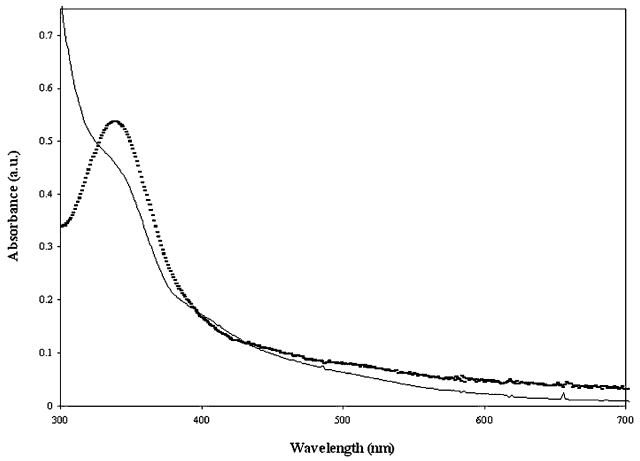

Fig. 3 Optical absorption spectra of an aqueous $[PdCl_4]^{2-}$ solution (dotted line) and a suspension of Pd/TOAB nanoparticles in toluene (solid line).

Vis absorbance profile shown by Pd nanoparticle suspensions in toluene does not show any surface plasmon band, in agreement with calculation of the extinction coefficients by means of the standard Mie theory.[41] This is due to both the very small particle size and the extension of interband transitions into the visible region.

The FT-IR spectrum (Fig. 4) mainly shows the bands associated with TOAB, without any differences between the IR spectra of samples A and B. The peaks corresponding to methylene antisymmetric (d^-) and symmetric (d^+) vibration modes at 2922 and 2852 cm^{-1}, respectively, as well as the methyl stretching mode at 2951 cm^{-1} are clearly seen. These bands can be used to determine the orientation and integrity of the methylene chains.[42–44] In the present case the position of the peak arising from methylene groups and the increase in intensity, relative to the methyl stretching peak, indicate that the structural integrity of the octyl group is maintained, without a significant density of defects in the chains, during formation of the nanoparticles and that solvent entrapment does not play a significant role.

Electron microscopy. Fig. 1 shows representative TEM images and histograms of sample A in toluene (Fig. 1 top) and upon transfer into water (Fig. 1 middle). It should be realised that in both media the sample mainly contains spherical nanoparticles with sizes below 1 nm and a narrow size distribution, indicating that very small nanoparticles can be synthesised in toluene and no agglomeration occurs during the transfer from toluene into water.

The larger nanoparticles (around 3.5 nm), sample B, were examined by HRTEM, showing fringes separated by 2.27 Å (Fig. 5(left)). The corresponding fast Fourier transform (FFT) shown in Fig. 5(right) reveals amplitude maxima (spots) representing the lattice periodicities for interlayer distances of 2.27 Å and 2.00 Å, in good agreement (within experimental error) with those calculated from the 76148 ICSD card for palladium, 2.244 Å and 1.944 Å for (111) and (002) lattice planes, respectively.

Thermal stability. The tetraoctylammonium (TOA)-capped palladium nanoparticles are stable at room temperature for a few weeks and for several months at low temperature (around 5 °C). The stability of these systems was also studied at higher

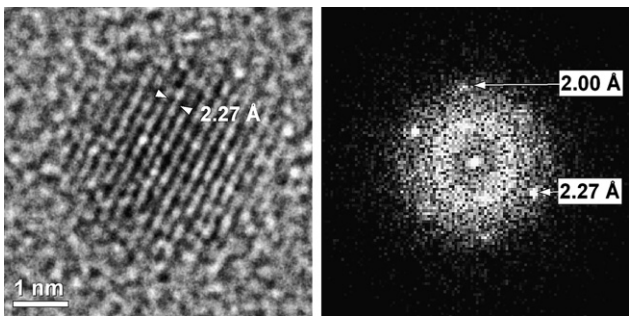

Fig. 5 (Left) HRTEM image showing the fringes of the palladium nanoparticles (sample B). (Right) Fast Fourier transform revealing the lattice periodicities of the palladium nanoparticles.

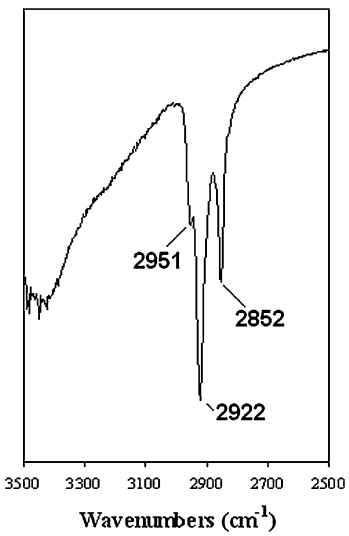

Fig. 4 KBr diluted FT-IR spectrum of solid palladium nanoparticles capped with TOAB (sample A).

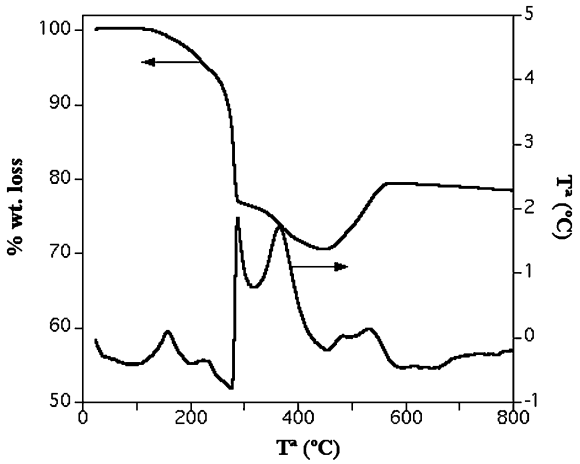

Fig. 6 TGA (above) and DTA (below) data for the solid sample A palladium nanoparticles.

temperatures through thermogravimetric analysis of the solid samples precipitated from ethanol. The TGA profile for the Pd nanoparticle–TOA system is shown in Fig. 6. No differences were observed between the TGA profiles of samples A and B, except for the total loss. In the first analysis two prominent losses are distinguished. However, a more detailed examination allows three losses to be differentiated: two starting at 100 and 200 °C and a third one at 330 °C, accounting for a total loss of 29.5% for sample A and 22.2% for sample B, which could be tentatively attributed to desorption of TOA from the surface of the palladium nanoparticles. However, taking into account that the first loss is endothermic and prolonged over a broad range of temperatures, it seems more appropriate to consider it as arising from desorption of solvent molecules (toluene) entrapped between the capping agent units. Making this assumption, one obtains that the amount of solvent is 2.7% and 4.0% for sample A and B, respectively. Finally, at 450 °C two exothermic peaks were identified, corresponding to oxidation of palladium nanoparticles, as a consequence of complete decomposition of the protective TOA layer.

X-Ray photoelectron spectroscopy. This technique provides information on the chemical state and can thus be used to distinguish between Pd metal and PdO. In this work, XPS is used to study the chemical composition of the Pd nanoparticles, to determine the amount of Pd that was oxidised to palladium oxide during the synthesis. A high resolution XPS Pd 3d spectrum for the palladium nanoparticles in dried sample A is shown in Fig. 7. One can clearly distinguish the characteristic $3d_{5/2}$ and $3d_{3/2}$ peaks for Pd(0) at 333.8 and 339.2 eV respectively and also those for Pd(II) at 335.9 and 341.4 eV. These results clearly indicate that part of the palladium is oxidised to palladium oxide (in sample A 45.8 at.% is PdO and for sample B the PdO is 10.7 at.%), likely during the step of palladium nanoparticle formation, generating an oxide shell surrounding the metal cluster. This phenomenon was described by Litran *et al.*[45] for the case of palladium nanoparticles protected by tetraalkylammonium with large alkyl groups as capping agents.

Magnetic properties

The onset of ferromagnetism in normally non-magnetic materials, like Pd and late 4d transition metals, and metal oxide nanostructures,[46] is attracting great attention in the magnetism community. In the case of Pd, ferromagnetism has been evidenced in samples prepared as nanoparticles or as thin films. Thus, Taniyama *et al.* found surface ferromagnetism in gas-evaporated Pd nanoparticles with average radius below 7 nm.[47] Later on, Litran *et al.* found hysteresis loops at room temperature for alkylammonium[48] and thiol[49] capped Pd nanoparticles in the size range between 1.2 and 2.4 nm.[45] More recently we have also observed room-temperature ferromagnetism in well-insulated Pd nanoparticles of *ca.* 2.4 nm surrounded by a small Pd oxide shell and encapsulated within an apoferritin cavity.[50] In these nanoparticles two different mechanisms have been proposed to account for the observed magnetic behaviour: One is related to the structural and electronic factors increasing the density of states of Pd just below the Fermi level (change in the crystal packing, local symmetry changes at twin boundaries, surface anisotropy induced by reduction in coordination number). The other is due to the electronic changes induced at the surface of the nanoparticle by the presence of bonded atoms (S, O) that are able to increase the 4d density of holes at the Pd site and to localize a magnetic moment.[45]

As these magnetic phenomena are rather new and controversial and very few examples are known so far, it seemed of interest to us to study the magnetic properties of the Pd nanoparticles synthesized in the present work. The alkylammonium capping on these nanoparticles is similar to that used by Litran *et al.* Still, while these authors used alkylammonium radicals of lengths C4 and C12, in the present work we used the C8 radical. We focused on the samples showing the largest size (sample B), as well as that showing the smallest size (sample A). The magnetic properties of these two samples after subtracting the diamagnetic contributions are shown in ESI† (sample A) and Fig. 8 (sample B). Sample B shows hysteresis loops at all temperatures between 2 and 300 K, indicating permanent magnetism even at room temperature. The hysteresis loops do not vary much with temperature. In fact, the values at 5 T vary from 0.002 to 0.0015 BM per Pd atom upon increasing the temperature from 2 K to 300 K. This small dependence of the magnetic moment with the temperature in the M vs. H plots suggests that magnetism is dominated by ferromagnetic entities. On the other hand, the magnetization at high fields is far from saturation. Thus, above 1 T a linear increase in the M vs. H curves was observed at all temperatures. This behaviour is indicative of the presence of negligible amounts of superparamagnetic and paramagnetic

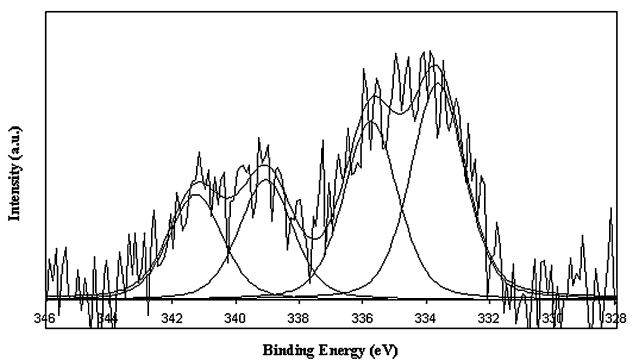

Fig. 7 XPS spectrum of a solid sample A of TOA-capped Pd nanoparticles.

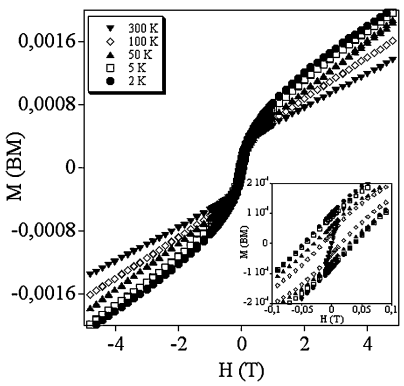

Fig. 8 Magnetisation hysteresis loops for Pd nanoparticles (sample B) at 2, 5, 50, 100, and 300 K.

contributions which coexist with the dominant ferromagnetic entities. These minor contributions might arise from Pd nanoparticles having low blocking temperatures and from the presence of residual paramagnetic centres (paramagnetic impurities, some Pd moments coming from the core of the nanoparticle, etc.). By extrapolating at zero field the high field magnetization, a permanent magnetic moment close to 0.4×10^{-3} BM per palladium atom is obtained at room temperature. Such a low value seems to indicate that only a small fraction of atoms exhibit a permanent magnetic moment and ferromagnetism. This value is slightly smaller than that reported by Hernando[49] and by us[50] for Pd nanoparticles of *ca.* 2.4 nm size surrounded by a layer of PdO (*ca.* 10^{-3} BM per Pd) Another parameter of interest is the coercive field. A decrease in H_c from 470 Oe at 2 K to 15 Oe at 300 K was obtained. This is indicative of the presence of blocked ferromagnetic nanoparticles having the blocking temperature near room temperature.

In contrast to sample B, the sub-nanometric particles (sample A) exhibit a much more pronounced temperature dependence in the M vs. H curves ESI†), in particular below 100 K. Thus, the low temperature curves are dominated by a paramagnetic-type contribution, and although a ferromagnetic component is observed even at 300 K, the value for the permanent magnetic moment is two orders of magnitude smaller than that obtained for sample B (*ca.* 5×10^{-5} BM per Pd). This extremely low value may not be intrinsic to the sample. In fact, it may be due to magnetic impurities of 3d or 4d transition elements. The small variation in the coercive field in the whole range of temperatures (*ca.* 90 Oe) indicates that these magnetic impurities get ordered at temperatures well above room temperature. Notice that the same amount of magnetic impurities (per Pd) are expected to be present in sample B, but they should give rise to a negligible magnetic signal as the permanent magnetism of this sample is two order of magnitude bigger.

Conclusions

In this work, experimental conditions for the synthesis of Pd nanoparticles were systematically varied in order to determine the key parameters involved in determining particle size and size distribution. As a result of these studies, palladium particles reaching sub-nanometric size (0.9 nm) and narrow size distribution (0.2 nm) were prepared.

The second important conclusion derived from this work deals with the magnetism of the Pd nanoparticles: permanent magnetism up to room temperature has been observed in the 3.5 nm nanoparticles, while this magnetism is almost lost when the size of the nanoparticles is reduced to 0.9 nm. The magnetism observed in the 3.5 nm Pd nanoparticles capped with tetraoctylammonium constitutes additional support for the onset of ferromagnetism in this kind of nanostructures. Notice that this unusual magnetic behaviour was first reported in Pd nanoparticles of 2.1–2.4 nm capped with other tetraalkylammonium salts having either shorter or longer lengths for the alkyl chains (C4 and C12 derivatives). These two systems exhibit clear differences in their magnetic behaviour. In fact, in the second case a complete oxidation of the nanoparticle surface occurs leading to a significant enhancement of the magnetization curve at low temperatures. In the present case, the intermediate length of the alkyl chain (C8) also appears to promote a certain oxidation of the nanoparticle surface. In fact, the extent of this oxidation (demonstrated by XPS) seems to indicate the formation of a core/shell structure for our nanoparticles, with a PdO monolayer at the surface. As previously proposed for similar 2 nm Pd nanoparticles,[45] the origin of the permanent magnetism observed in this kind of nanoparticles comes primarily from the surface Pd atoms located near the PdO shell. In this case, the formation of Pd–O bonds produces an increase in the density of holes at the 4d residual band of Pd, inducing the permanent magnetism observed.

Finally, the lack of ferromagnetism in the sub-nanometric Pd particles will deserve further attention in the future. The nanoparticles reported in this paper represent the lowest limit in size, as, according to this size, the core is formed by a cluster of 13 Pd atoms surrounded by a PdO shell. In a recent paper the study of Pd nanoparticles of 2 to 10 nm stabilized by the protective ligand trioctylphosphine has been reported.[51] In that paper it was suggested that magnetization increases with decreasing particle size, indicating the important role played by the surface Pd atoms. The loss of ferromagnetism in our sub-nanometric particles indicates that for very small sizes this tendency is no longer valid. The flexibility of the synthesis procedure described in this paper should enable the easy preparation of sub-nanometric monodispersed particles of various sizes using different capping molecules, controlling thus the oxidation at the surface of the Pd core, and therefore one should be able to study when the ferromagnetism is going to be observed. This work is currently under way.

Acknowledgements

This research has been funded by the Spanish Ministerio de Ciencia e Innovación (Projects CONSOLIDER-INGENIO in Molecular Nanoscience CSD2007-00010, MAT2007-61584 and CTQ2005-09385) and by the Generalidad Valenciana. A.R., J.G.M. and N.L. thank the Ministerio de Ciencia e Innovación for a Ramón y Cajal contract and PhD fellowship, respectively. B. Rodríguez-González from the CACTI of U. Vigo is acknowledged for carrying out the HRTEM measurements.

References

1 M. Faraday, *Philos. Trans. Royal Soc. London*, 1857, **147**, 145.
2 S. Chen and Y. Yang, *J. Am. Chem. Soc.*, 2002, **124**, 5280–5281.
3 C. J. Murphy and N. R. Jana, *Adv. Mater.*, 2002, **14**, 80–82.
4 L. A. Peyser, A. E. Vinson, A. P. Bartko and R. M. Dickson, *Science*, 2001, **291**, 103–106.
5 A. C. Templeton, W. P. Wuelfing and R. W. Murray, *Acc Chem Res*, 2000, **33**, 27–36.
6 X. Teng, D. Black, N. J. Watkins, Y. Gao and H. Yang, *Nano Lett.*, 2003, **3**, 261–264.
7 A. G. Tkachenko, H. Xie, D. Coleman, W. Glomm, J. Ryan, M. F. Anderson, S. Franzen and D. L. Feldheim, *J. Am. Chem. Soc.*, 2003, **125**, 4700–4701.
8 X. Zhang, M. A. Young, O. Lyandres and R. P. Van Duyne, *J. Am. Chem. Soc.*, 2005, **127**, 4484–4489.
9 C. N. R. Rao, G. U. Kulkarni, P. J. Thomas and P. P. Edwards, *Chem. Soc. Rev.*, 2000, **29**, 27–35.
10 H. Hahn and R. S. Averback, *J. Appl. Phys.*, 1990, **67**, 1113–1116.
11 Y. Li, J. Liu, Y. Wang and Z. L. Wang, *Chem. Mater.*, 2001, **13**, 1008–1014.
12 G. W. Rice, *ACS Sym. Ser.*, 1993, **530**, 273–278.

13 J. G. Brennan, T. Siegrist, P. J. Carroll, S. M. Stuczynski, L. E. Brus and M. L. Steigerwald, *J. Am. Chem. Soc.*, 1989, **111**, 4141–4143.
14 C. B. Murray, D. J. Norris and M. G. Bawendi, *J. Am. Chem. Soc.*, 1993, **115**, 8706–8715.
15 A. P. Alivisatos, *Science*, 1996, **271**, 933–937.
16 Y. Yin and A. P. Alivisatos, *Nature*, 2005, **437**, 664–670.
17 X. Wang, J. Zhuang, Q. Peng and Y. Li, *Nature*, 2005, **437**, 121–124.
18 M. H. Huang, S. Mao, H. Feick, H. Yan, Y. Wu, H. Kind, E. Weber, R. Russo and P. Yang, *Science*, 2001, **292**, 1897–1899.
19 X. Duan and C. M. Lieber, *Adv. Mater.*, 2000, **12**, 298–302.
20 A. M. Morales and C. M. Lieber, *Science*, 1998, **279**, 208–211.
21 I. G. Koo, M. S. Lee, J. H. Shim, J. H. Ahn and W. M. Lee, *J. Mater. Chem.*, 2005, **15**, 4125–4128.
22 M.-C. Daniel and D. Astruc, *Chem. Rev.*, 2004, **104**, 293–346.
23 J. Turkevich, P. C. Stevenson and J. Hillier, *Discuss. Faraday Soc.*, 1951, **No. 11**, 55–75.
24 G. Frens, *Nature (London), Physical Science*, 1973, **241**, 20–22.
25 J. Turkevich, R. S. Miner, Jr. and L. Babenkova, *J. Phys. Chem.*, 1986, **90**, 4765–4767.
26 D. N. Furlong, A. Launikonis, W. H. F. Sasse and J. V. Sanders, *J. Chem. Soc., Faraday Trans. 1*, 1984, **80**, 571–588.
27 M. Brust, M. Walker, D. Bethell, D. J. Schiffrin and R. Whyman, *J. Chem. Soc., Chem. Commun.*, 1994, 801–802.
28 D. I. Gittins and F. Caruso, *Angew. Chem., Int. Ed.*, 2001, **40**, 3001–3004.
29 M. Brust, J. Fink, D. Bethell, D. J. Schiffrin and C. Kiely, *J. Chem. Soc., Chem. Commun.*, 1995, 1655–1656.
30 J. R. Heath, C. M. Knobler and D. V. Leff, *J. Phys. Chem. B*, 1997, **101**, 189–197.
31 B. A. Korgel, S. Fullam, S. Connolly and D. Fitzmaurice, *J. Phys. Chem. B*, 1998, **102**, 8379–8388.
32 C. R. K. Rao, V. Lakshminarayanan and D. C. Trivedi, *Mater. Lett.*, 2006, **60**, 3165–3169.
33 H. Hirai, Y. Nakao and N. Toshima, *J. Macromol. Sci., Chem.*, 1979, **13**, 727–750.
34 Y. Wang and N. Toshima, *J. Phys. Chem. B*, 1997, **101**, 5301–5306.
35 I. Pastoriza-Santos and L. M. Liz-Marzan, *Langmuir*, 2002, **18**, 2888–2894.
36 C. Ducamp-Sanguesa, R. Herrera-Urbina and M. Figlarz, *J. Solid State Chem.*, 1992, **100**, 272–280.
37 P.-Y. Silvert, R. Herrera-Urbina, N. Duvauchelle, V. Vijayakrishnan and K. T. Elhsissen, *J. Mater. Chem.*, 1996, **6**, 573–577.
38 Y. Sun, B. Gates, B. Mayers and Y. Xia, *Nano Letters*, 2002, **2**, 165–168.
39 Y. Sun, Y. Yin, B. T. Mayers, T. Herricks and Y. Xia, *Chem. Mater.*, 2002, **14**, 4736–4745.
40 J. A. Creighton and D. G. Eadon, *J. Chem. Soc., Faraday Trans.*, 1991, **87**, 3881–3891.
41 C. F. Bohren and D. R. Huffman, *Absorption and Scattering of Light by Small Particles*, John Wiley and Sons, Inc., New York, 1983.
42 R. G. Nuzzo, F. A. Fusco and D. L. Allara, *J. Am. Chem. Soc.*, 1987, **109**, 2358–2368.
43 R. G. Nuzzo, L. H. Dubois and D. L. Allara, *J. Am. Chem. Soc.*, 1990, **112**, 558–569.
44 M. D. Porter, T. B. Bright, D. L. Allara and C. E. D. Chidsey, *J. Am. Chem. Soc.*, 1987, **109**, 3559–3568.
45 R. Litran, B. Sampedro, T. C. Rojas, M. Multigner, J. C. Sanchez-Lopez, P. Crespo, C. Lopez-Cartes, M. A. Garcia, A. Hernando and A. Fernandez, *Phys. Rev. B*, 2006, **73**, 054404.
46 M. A. Garcia, J. M. Merino, E. Fernandez Pinel, A. Quesada, J. De la Venta, M. L. Ruiz Gonzalez, G. R. Castro, P. Crespo, J. Llopis, J. M. Gonzalez-Calbet and A. Hernando, *Nano Lett.*, 2007, **7**, 1489–1494.
47 T. Taniyama, E. Ohta and T. Sato, *Europhy. Lett.*, 1997, **38**, 195–200.
48 B. Sampedro, P. Crespo, A. Hernando, R. Litran, J. C. Sanchez Lopez, C. Lopez Cartes, A. Fernandez, J. Ramirez, J. Gonzalez Calbet and M. Vallet, *Phys. Rev. Lett.*, 2003, **91**, 237203.
49 A. Hernando, B. Sampedro, R. Litran, T. C. Rojas, J. C. Sanchez-Lopez and A. Fernandez, *Nanotechnology*, 2006, **17**, 1449–1453.
50 M. Clemente-Leon, E. Coronado, A. Soriano-Portillo, N. Galvez and J. M. Dominguez-Vera, *J. Mater. Chem.*, 2007, **17**, 49–51.
51 S. Angappane, J. Park, Y. Jang, T. Hyeon and J. G. Park, *J. Phys.: Condensed Matter*, 2008, **20**, 295209.

